



1 **Observation of atmospheric peroxides during Wangdu Campaign**

2 **2014 at a rural site in the North China Plain**

3 **Yin Wang, Zhongming Chen, Qinqin Wu, Hao Liang, Liubin Huang, Huan Li,**

4 **Keding Lu, Yusheng Wu, Huabin Dong, Limin Zeng, and Yuanhang Zhang**

5 State Key Laboratory of Environmental Simulation and Pollution Control, College of

6 Environmental Sciences and Engineering, Peking University, Beijing 100871, China

7 *Correspondence to:* Zhongming Chen (zmchen@pku.edu.cn)

8 **Abstract**

9 Measurements of atmospheric peroxides were made during Wangdu Campaign 2014 at
10 Wangdu, a rural site in the North China Plain (NCP) in summer 2014. The predominant
11 peroxides were detected to be hydrogen peroxide (H_2O_2), methyl hydroperoxide (MHP)
12 and peroxyacetic acid (PAA). The observed H_2O_2 reached up to 11.3 ppbv, which was
13 the highest value compared with previous observations in China at summer time. A box
14 model simulation based on the Master Chemical Mechanism and constrained by the
15 simultaneous observations of physical parameters and chemical species was performed
16 to explore the chemical budget of atmospheric peroxides. Photochemical oxidation of
17 alkenes was found to be the major secondary formation pathway of atmospheric
18 peroxides, while contributions from alkanes and aromatics were of minor importance.
19 The comparison of modelled and measured peroxide concentrations revealed an
20 underestimation during biomass burning events and an overestimation on haze days,
21 which were ascribed to the direct production of peroxides from biomass burning and
22 the heterogeneous uptake of peroxides by aerosols, respectively. The strengths of the
23 primary emissions from biomass burning were on the same order of the known
24 secondary production rates of atmospheric peroxides during the biomass burning events.
25 The heterogeneous process on aerosol particles was suggested to be the predominant
26 sink for atmospheric peroxides. The atmospheric lifetime of peroxides on haze days in
27 summer in the NCP was about 2–3 hours, which is in good agreement with the



28 laboratory studies. Further comprehensive investigations are necessary to better
29 understand the impact of biomass burning and heterogeneous uptake on the
30 concentration of peroxides in the atmosphere.

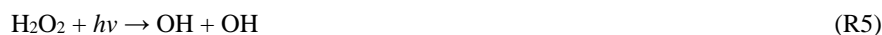
31 **1 Introduction**

32 Atmospheric peroxides, including hydrogen peroxide (H_2O_2) and organic peroxides
33 (ROOH), are vital oxidants present in the gaseous, aqueous and particulate phase in the
34 atmospheric chemical processes. They serve as temporary reservoirs for HO_x radicals,
35 contributing to the atmospheric oxidation capacity (Reeves and Penkett, 2003).
36 Peroxides also participate in the conversion of S(IV) to S(VI) in the aqueous phase,
37 leading to the acid precipitation and the formation of secondary sulfate (SO_4^{2-}) aerosols
38 in the troposphere (Calvert et al., 1985; Stein and Saylor, 2012). Furthermore,
39 atmospheric peroxides are considered as the key components of secondary organic
40 aerosol (SOA), which play a significant role in the formation and duration of haze
41 pollution (Kroll and Seinfeld, 2008; Ziemann and Atkinson, 2012; Li et al., 2016). In
42 addition, it has been suggested that atmospheric peroxides are toxic to ecosystem and
43 may be the critical pollutants of forest decline (Hellpointner and G äb, 1989; Chen et al.,
44 2010). More importantly, peroxides in the particle phase have been found to act as
45 reactive oxygen species (ROS) and result in adverse influence on human health (Ayres
46 et al., 2008).

47 The concentrations of atmospheric peroxides are determined by their production and
48 destruction. The known formation pathways of peroxides in the atmosphere are primary
49 emissions, for instance, biomass burning (Lee et al., 1997, 1998; Yokelson et al., 2009),
50 and secondary sources such as peroxy radical self/cross reactions and the ozonolysis of
51 unsaturated volatile organic compounds (VOCs), as shown in Reaction (R1, R2) and
52 (R3, R4), respectively (Hewitt and Kok, 1991; Neeb et al., 1997; Sauer et al., 2001;
53 Chao et al., 2015; Winiberg et al., 2016). Additionally, atmospheric aqueous reactions
54 in the bulk solution or on the surface of wet particles coupled with subsequent release
55 to the gas phase could also generate peroxides in the troposphere (Wang et al., 2012;
56 Liang et al., 2013a; Zhao et al., 2013a). The typical removal pathways of peroxides in



57 the atmosphere are photolysis (R5, R6), reaction with OH radicals (R7, R8) and
58 physical deposition (Atkinson et al., 2006; Sander et al., 2011; Nguyen et al., 2015).
59 Heterogeneous uptake by atmospheric aerosols is recognized as another significant sink
60 for peroxides in the troposphere, especially in dusty and polluted urban areas (Zhao et
61 al., 2013b; Wu et al., 2015).



62 In the past years, a number of field observations, laboratory studies and modelling
63 research have been carried out to investigate the abundance and behavior of peroxides
64 in the atmosphere (Chen et al., 2008; Mao et al., 2010; Huang et al., 2013; Liang et al.,
65 2013a; Sarwar et al., 2013; Epstein et al., 2014; Fischer et al., 2015; Khan et al., 2015).
66 Hydrogen peroxide (H_2O_2), hydroxymethyl hydroperoxide (HMHP, HOCH_2OOH),
67 methyl hydroperoxide (MHP, CH_3OOH) and peroxyacetic acid (PAA, $\text{CH}_3\text{C}(\text{O})\text{OOH}$)
68 are generally determined to be the principal peroxide compounds in the troposphere
69 with their concentrations ranging from pptv (parts per trillion by volume) to ppbv (parts
70 per billion by volume) (Lee et al., 2000; He et al., 2010; Zhang et al., 2010, 2012).
71 However, to date, there have been limited studies concerned with atmospheric
72 peroxides in the regions primarily affected by anthropogenic sources such as the North
73 China Plain (NCP), which is a typical region with frequent biomass burning and
74 suffering from serious haze pollution in China (Tao et al., 2012; Huang et al., 2014).
75 Few numerical simulations focused on atmospheric peroxides in the NCP are conducted
76 to examine whether the models can reproduce the observations of peroxides (Liang et
77 al., 2013a). The impact of biomass burning and high aerosol loading on the atmospheric
78 chemistry of peroxides over such a polluted region is poorly understood. Therefore, this



79 work was carried out in order to make an endeavor to fill in these research gaps.

80 In this study, we present a novel dataset of atmospheric speciated peroxides and
81 explore their atmospheric chemistry at a rural site, Wangdu, which represents regional
82 air pollution conditions of the NCP during Wangdu Campaign 2014. Given the diversity
83 of emission sources and chemical transformation of atmospheric peroxides over this
84 region, it is challenging to analyze the phenomena and understand the primary emission
85 and secondary formation of peroxides in the atmosphere during this field observation.
86 However, with the continuous measurements of atmospheric peroxides, physical
87 parameters and other chemical species performed simultaneously, a quantitative
88 assessment of the budget of atmospheric peroxides can be carried out employing the
89 zero-dimensional model based on Master Chemical Mechanism (MCM) and
90 constrained by observed meteorological parameters and trace gases, which provides a
91 good opportunity to comprehensively facilitate our knowledge of the chemistry of
92 atmospheric peroxides in the NCP. As far as we know, this is the first study to test
93 whether current atmospheric peroxides related chemistry could explain the field
94 observation in the rural area of the NCP. Through the comparison between measurement
95 and simulation, our aim is to investigate the role of biomass burning and heterogeneous
96 uptake on aerosols in the concentration of atmospheric peroxides, which helps to
97 develop more robust mechanism in the model.

98 **2 Experiments**

99 **2.1 Measurement site**

100 Measurements of atmospheric peroxides were performed at Wangdu site (38.66 °N,
101 115.20 °E) in Baoding city, Hebei Province, a rural supersite for the Wangdu Campaign
102 2014 situated in the northwest of the NCP, about 200 km southwest of the mega-city
103 Beijing. The surrounding regions of Wangdu site are mainly agricultural fields. There
104 are almost no industries near this site. During the summer season, the air pollution is
105 caused by the primary emission from biomass burning and secondary formation
106 including photochemical and heterogeneous processes. The instruments were placed in
107 a container with the sampling inlet approximately 5 m above the ground. The



108 continuous observation of atmospheric peroxides was conducted from 4 June to 7 July
109 2014.

110 **2.2 Measurement methods**

111 **2.2.1 Measurement method for atmospheric peroxides**

112 Atmospheric peroxide concentrations were investigated by an automated on-site high
113 performance liquid chromatography (HPLC) with post-column enzyme derivatization
114 and detected by fluorescence spectroscopy. Air samples were pumped through a glass
115 scrubbing coil maintained at a controlled temperature of about 4 °C to collect the
116 peroxides in the atmosphere. The flow rate of air samples was set to be 2.7 standard L
117 min⁻¹. The stripping solution, 5 × 10⁻³ M H₃PO₄ in water was delivered into the
118 scrubbing coil collector. The flow rate of stripping solution was set to be 0.2 mL min⁻¹.
119 Once the air samples mixed with the stripping solution in the collector, the mixture was
120 carried by the mobile phase containing 5 × 10⁻³ M H₃PO₄ at 0.5 mL min⁻¹ and injected
121 into HPLC. The peroxide components were separated after the mixture passed through
122 HPLC column. With the catalysis of Hemin at ~40 °C, the derivatization reaction
123 between peroxide components and para-hydroxyphenylacetic acid (PHPAA) produced
124 the fluorescent matter that can be quantified by fluorescence detector. In this work,
125 atmospheric peroxides were measured every 20 min. The collection efficiencies for
126 hydrogen peroxide and organic peroxides were determined to be 100% and 85%,
127 respectively. The detection limit of peroxides in the gas phase was about 10 pptv.

128 The interference of SO₂ on the sampling was estimated using the theoretical
129 thermodynamic and kinetic analysis presented in Hua et al. (2008). Considering the rate
130 constant for reaction between peroxides and S(IV) reported by Ervens et al. (2003) and
131 the mean level of SO₂ was 7.0 ± 7.0 ppbv during the campaign, the negative artifact
132 caused by SO₂ interference for peroxides was calculated to be less than 15%. The
133 influence of ambient relative humidity (RH) on the measurement of atmospheric
134 peroxides was calculated following the method introduced by Liang et al. (2013b). The
135 change of the concentration of atmospheric peroxides after this calibration is less than
136 10%. Here, we did not correct the observational data for any artifacts due to the



137 uncertainties from the theoretical estimation of peroxides loss that possibly result in
138 new errors. The uncertainty of our observational data is estimated to be ~15%. Further
139 details about our measurement method for atmospheric peroxides can be obtained from
140 Hua et al. (2008).

141 **2.2.2 Measurement methods for other pollutants and parameters**

142 During Wangdu Campaign 2014, SO₂, CO, NO/NO₂ and O₃ were measured
143 concurrently at this supersite using a suite of commercial instruments (Thermo 43i, 42i,
144 48i and 49i). HONO was measured every 2 min with a LOng Path Absorption
145 Photometer (LOPAP) (Liu et al., 2016). C₂–C₁₀ non-methane hydrocarbons (NMHCs)
146 were analyzed with a time resolution of 60 min by a custom-built online VOC analyzer
147 using automated gas chromatography (GC) coupled with flame ionization detector (FID)
148 or mass spectrometry (MS) technique (Wang et al., 2014). OH and HO₂ radicals were
149 measured by laser-induced fluorescence (LIF) spectroscopy. Size distributions of
150 aerosols (PM₁₀) were determined every 10 min with a Twin Differential Mobility
151 Particle Sizer (TDMPs) and an Aerodynamic Particle Sizer (APS) to calculate dry
152 particle surface area concentrations (S_a). Hygroscopic growth factor, f (RH), which is
153 defined as the ratio of scattering coefficient for ambient aerosol to scattering coefficient
154 for dry aerosol, was derived from the integrating nephelometer (Liu, 2015).
155 Measurements of the mass concentration of PM_{2.5} were obtained by TEOM 1400A
156 analyzer. Photolysis frequencies were derived from a spectro-radiometer (Bohn et al.,
157 2008). Meteorological parameters including ambient temperature, relative humidity
158 (RH), pressure, wind speed, wind direction and rainfall were monitored continuously
159 by a weather station. The uncertainties (1σ) in these measurements are estimated as 5%
160 for NO, O₃, and CO, 10% for H₂O, NO₂, HONO, NMHCs, and solar radiation, and 20%
161 for S_a .

162 **2.3 Model description**

163 A zero-dimensional box model using a near-explicit mechanism, MCM Version 3.3.1
164 (<http://mcm.leeds.ac.uk/MCM/>) (Jenkin et al., 1997, 2003; Saunders et al., 2003; Jenkin
165 et al., 2015) was employed to examine the influence of biomass burning and



166 heterogeneous uptake on the budget of atmospheric peroxides. MCMv3.3.1 describes
167 the degradation of 143 VOCs, leading to about 5800 species and 17000 reactions. In
168 the current study, we extracted a subset of MCMv3.3.1 containing the reactions of
169 atmospheric oxidants with measured VOCs and subsequent chemical products.
170 Measurements of NO/NO₂, CO, O₃, HONO, NMHCs, temperature, pressure and H₂O
171 were used as inputs to constrain the model calculations. The model ran with a 5-min
172 time step and a spin-up time of 2 days to reach a steady state. Photolysis frequencies
173 were calculated by the Tropospheric Ultraviolet and Visible (TUV, version 5.2) model
174 (Madronich, 2002), and further rescaled with the measured $j(\text{NO}_2)$. Dry deposition
175 velocities of trace gases in our box model were parameterized as V_d/h (Seinfeld and
176 Pandis, 2006), where V_d is the dry deposition rate of species and h is the height of
177 planetary boundary layer (PBL). Dry deposition rates of HNO₃, PANs, organic nitrates,
178 H₂O₂, organic peroxides and aldehydes incorporated in the model were set as 2.0×10^{-5}
179 s^{-1} , $5.0 \times 10^{-6} \text{ s}^{-1}$, $1.0 \times 10^{-5} \text{ s}^{-1}$, $1.0 \times 10^{-5} \text{ s}^{-1}$, $5.0 \times 10^{-6} \text{ s}^{-1}$ and $1.0 \times 10^{-5} \text{ s}^{-1}$, respectively
180 at the PBL height of 1 km (Zhang et al., 2003; Emmerson et al., 2007; Lu et al., 2012;
181 Guo et al., 2014; Li et al., 2014c; Liu et al., 2015; Nguyen et al., 2015). The PBL height
182 over Wangdu during this campaign was derived from the hybrid single-particle
183 lagrangian integrated trajectory (HYSPLIT) model (Draxler and Rolph, 2012), which
184 varied between about 300 m at midnight and over 3000 m at noon. The uncertainty of
185 our model calculation derives from the uncertainty of observational data. The total
186 uncertainty in the model was estimated from the errors of all input parameters using
187 error propagation, which is similar to the method that can be found in Hofzumahaus et
188 al. (2009). On average, the modelled concentration of atmospheric peroxides had an
189 uncertainty of approx. 40%. In the present study, to explore the impact of the
190 heterogeneous process on the concentration of atmospheric peroxides, our box model
191 is extended with the aerosol uptake of peroxides. The pseudo-first-order rate constant
192 for the heterogeneous uptake of peroxides on ambient aerosols is parameterized as
193 follows:

$$194 \quad k = \frac{1}{4} \gamma \cdot v \cdot S_{\text{aw}} \quad (1)$$



195 (Jacob, 2000), where γ is the uptake coefficient, v is the mean molecular velocity, S_{aw}
196 is the aerosol surface concentration corrected by the measured hygroscopic factor, $f(\text{RH})$
197 that could be expressed as $S_{aw} = S_a \times f(\text{RH})$.

198 3 Results and Discussion

199 3.1 General observations

200 The concentrations of peroxides in the atmosphere were measured continuously from 4
201 June to 7 July 2014. The predominant peroxides over Wangdu included H_2O_2 , MHP and
202 PAA. Time series for atmospheric peroxides during Wangdu Campaign 2014 are
203 illustrated in Fig. 1. The statistical data about the observed concentration of atmospheric
204 peroxides are summarized and given in Table 1. It should be noted that values below
205 the detection limit (D.L.) of our instrument were replaced by the corresponding D.L. in
206 Fig. 1, Fig. 2 and statistical calculations. In this study, H_2O_2 accounted for ~70% of
207 total detected peroxides ($\text{H}_2\text{O}_2 + \text{MHP} + \text{PAA}$). However, in our previous work, H_2O_2
208 contributed not more than 30% of total peroxides in the atmosphere over urban Beijing
209 at the summer time of 2010 and 2011 (Liang et al., 2013b). This might be caused by
210 the difference on the production and destruction of atmospheric peroxides between two
211 sites. MHP and PAA were determined to be about 20% and 5% of total peroxides over
212 Wangdu, respectively, which is similar to the results of other rural sites in China from
213 our previous investigations (Zhang et al., 2010, 2012).

214 During this campaign, there were four severe pollution episodes at Wangdu site as
215 follows: Episode 1 (4 June–6 June), Episode 2 (12 June–17 June), Episode 3 (29 June–
216 3 July) and Episode 4 (5 July–7 July) with elevated average $\text{PM}_{2.5}$ concentrations (75
217 $\mu\text{g m}^{-3}$, $92 \mu\text{g m}^{-3}$, $79 \mu\text{g m}^{-3}$ and $99 \mu\text{g m}^{-3}$, respectively). In Episode 1, H_2O_2 , MHP
218 and PAA were observed up to 11.3 ppbv, 0.9 ppbv and 1.5 ppbv, respectively. The
219 maximum H_2O_2 concentration on 5 June was the highest value so far among the
220 previously reported observations in urban, suburban and rural areas in China at summer
221 time. The possible reason for this peak concentration at Wangdu site could be the
222 primary emission from biomass burning combined with the secondary formation by the
223 intense photochemical process. Nevertheless, owing to the lack of supporting data for



224 other pollutants and parameters, it is difficult to identify the relative contributions of
225 biomass burning versus photochemical formation to the burst of atmospheric peroxides
226 on 5 June. In Episode 2, there was widespread and intensive biomass burning in the
227 NCP as this observation period covered the local wheat harvest season. The sudden
228 raise of atmospheric peroxides was observed and further discussed in Sect. 3.3. In
229 Episode 3, there was a substantial decline of H₂O₂, MHP and PAA level during this
230 typical haze event compared with the foregoing two episodes, which can be ascribed to
231 the heterogeneous uptake of peroxides on atmospheric aerosols on haze days over
232 Wangdu (See Sect. 3.4). In Episode 4, Wangdu was significantly impacted by the
233 regional transport (Ye, 2015). The concentrations of atmospheric peroxides remained
234 relatively low compared with the other three episodes. In addition to the above-
235 mentioned episodes, it was relatively clear between 8 June and 11 June and 27 June and
236 28 June, with mean PM_{2.5} concentrations under 40 µg m⁻³. The intermittent
237 thunderstorm activities occurred from 19 June to 25 June that caused the electric power
238 failure and several data gaps.

239 3.2 Peroxide simulation

240 In this study, we employed a box model based on the MCMv3.3.1 to simulate H₂O₂,
241 MHP and PAA concentrations. Here, to explore the atmospheric chemistry of peroxides
242 on non-haze, biomass burning and haze days, the observational data from 8 June to 11
243 June (Phase I), from 15 June to 17 June (Phase II) and from 29 June to 3 July (Phase
244 III) in 2014 were selected as phase of interest and analyzed in detail using box model
245 in the following sections. The temporal variations of meteorological parameters,
246 chemical species and atmospheric peroxides for these three phases are displayed in Fig.
247 2. The observed and calculated levels of atmospheric peroxides for the three phases are
248 illustrated in Fig. 3. During these case study phases, 75% of the wind speed data were
249 $\leq 2.2 \text{ m s}^{-1}$ and the mean value was 1.6 m s^{-1} . It has been shown that the atmospheric
250 lifetimes of peroxides are on the order of several hours as reported previously (He et
251 al., 2010; Wu et al., 2015), implying that the effect of regional transport or dilution on
252 the concentrations of atmospheric peroxides was of little significance over Wangdu.



253 Hence, the regional-scale transport can be excluded in our box model and the budgets
254 of peroxides are, to a large extent, dependent on local chemical processes during the
255 observation. In the Phase I, as shown in Fig. 4, the model prediction had good
256 performance in the daytime (06:00–18:00 local time), which was 1–2 times higher than
257 the measurement results. This seems to be explained by the model-measurement
258 uncertainty. Similarly, a previous observation carried out at a suburban site also showed
259 reasonable model-measurement agreement in H_2O_2 level on sunny days (Guo et al.,
260 2014). The excellent description yielded by the model base case indicated that the
261 production and destruction of atmospheric peroxides on non-haze days were calculated
262 correctly based on the current understanding of atmospheric peroxide related chemistry.
263 However, the simulation in the nighttime (18:00–06:00 local time) during the Phase I
264 demonstrated an obvious overestimation compared to the observation by a factor of 4–
265 6 and up to an order of magnitude. This large discrepancy between calculated and
266 observed results is speculated to be resulted from the underestimation of sink terms as
267 the key precursors governing the formation of atmospheric peroxides are constrained
268 by the observation and the overestimation of source terms can be ruled out by assuming
269 that the chemical mechanisms of atmospheric peroxides are well-understood. It
270 coincides with the comparison of the simulated and observed H_2O_2 concentration over
271 urban Beijing, in which the explanation for the overprediction of H_2O_2 level on haze
272 days was thought to be the heterogeneous processes on liquid or solid particles that
273 were missing from the current atmospheric chemistry model (Liang et al., 2013b).
274 Considering the high aerosol loading in the NCP and the higher aerosol surface area
275 concentration at nighttime than that at daytime in the Phase I, we believe that the
276 missing sink for atmospheric peroxides in the model base case is probably
277 heterogeneous uptake of peroxides occurring on aerosols. The strength of the missing
278 sink for H_2O_2 , MHP and PAA were estimated to be 0.24, 0.09, 0.03 ppbv h^{-1} on average,
279 respectively, which was on the same order of magnitude as the known loss rates of
280 atmospheric peroxides during the Phase I. In the Phase II, the comparison of the
281 modelled and measured peroxide concentrations in Fig. 3 displays that the observed
282 magnitude of atmospheric peroxides was unexpectedly large, indicating a missing



283 source for peroxides. Such a strong imbalance was found only in the Phase II during
284 the whole campaign, and the measurement-to-model ratio based on the model case was
285 up to a factor of 7 for MHP on 17 June, which was much higher than the measurement
286 and model errors. In the past, the higher-than-expected concentrations of atmospheric
287 peroxides have also been reported by Lee et al. (1997), in which H₂O₂, MHP, PAA and
288 other organic peroxides levels elevated near biomass burning plumes. Given the
289 frequent fire emissions in the NCP during the Phase II that are quite similar to the
290 conditions in Lee et al. (1997), it appears that the significant mismatch can be attributed
291 to the direct production from biomass burning (See Sect. 3.3). In the Phase III, the
292 calculated values in the model base case showed a general tendency to strongly
293 overestimate the observed values (Fig. 3). As there was a typical haze event during the
294 Phase III, the model-measurement imbalance was probably due to the missing sink for
295 atmospheric peroxides, which was the same deficiency in the model as that in the Phase
296 I. It can be seen in Fig. 3 that with the inclusion of heterogeneous reactions on aerosol
297 particles, the simulated concentrations of atmospheric peroxides were apparently
298 improved, which is further quantified in Sect. 3.4.

299 Before exploring the impact of biomass burning and heterogeneous uptake on the
300 chemistry of atmospheric peroxides, we performed a model test by implementing the
301 newly proposed chemical mechanisms for CH₃C(O)O₂ and CH₃O₂ related chemistry in
302 MCMv3.3.1, as listed in Table 2. The rate constant and the branching ratios of the
303 CH₃C(O)O₂ + HO₂ reaction that was the major pathway for the formation of PAA in
304 this model scenario were modified according to the recent laboratory study conducted
305 by Winiberg et al. (2016). Additionally, we also incorporated the reaction between
306 CH₃O₂ radicals and OH radicals that has as yet seldom been involved in atmospheric
307 chemistry model because it was recognized as an important sink for CH₃O₂ radicals
308 with non-negligible effect on subsequent formation of MHP under remote conditions
309 by Bossolasco et al. (2014) and Fittschen et al. (2014), in spite of the fact that the
310 reaction product is still unknown. As shown in Fig.3, the model run containing newly-
311 proposed mechanisms did not have a remarkable influence on the simulated results of
312 H₂O₂ in comparison to the model base case. But a slight difference of up to ~20%



313 between calculated and observed MHP can be noted at night, resulting from the
314 additional removal pathway of CH_3O_2 radicals from the noon to the sunset. The increase
315 of over 70% in rate constant and the reduction of about 10% in the branching ratio of
316 the reaction $\text{CH}_3\text{C}(\text{O})\text{O}_2 + \text{HO}_2 \rightarrow \text{CH}_3\text{C}(\text{O})\text{OOH}$ generated systematically 1.5 times
317 higher PAA concentration in this model scenario than that in the model base case.
318 Nevertheless, although the modelled PAA during the Phase II can be raised close to the
319 level of the observation, the concentrations of atmospheric peroxides were not fully
320 captured by the model with the implementation of newly proposed mechanisms (Fig.
321 3). Moreover, the resulting MHP and PAA values still agreed with the measurements
322 in the range of their errors. Thus, we can conclude that the additional chemical
323 mechanisms embedded in the model only have a marginal impact that is not sufficient
324 to match the observed peroxides in the atmosphere. The efficient source or sink for the
325 reproduction of the observation will be deeply investigated below.

326 As outlined in the introduction, the source of H_2O_2 , MHP and PAA are the direct
327 emission from biomass burning and the photochemical oxidation of VOC precursors
328 via HO_2 , CH_3O_2 and $\text{CH}_3\text{C}(\text{O})\text{O}_2$ formation. However, it is still difficult to determine
329 the contributions of VOC precursors at a species level. Here, to gain further insight into
330 the secondary chemical transformation of atmospheric peroxides at Wangdu site, the
331 sensitivity study with an indirect approach adopted referring to the relative incremental
332 reactivity (RIR) concept for ozone formation in Cardelino and Chameides (1995) was
333 utilized to track out the major VOC precursors of atmospheric peroxides and assess
334 their roles by the numerical model with the application of the MCMv3.3.1 that can
335 describe the explicit degradations of VOC species and quantify their contributions
336 individually. In this work, the definition of RIR is the ratio of reduction in the
337 production rates of atmospheric peroxides to the reduction of VOC precursor
338 abundances by 25% compared to the model base case, which can be regarded as a proxy
339 for the influence of a specific VOC on the *in-situ* formation of atmospheric peroxides.
340 The Phase I and Phase III were selected for the analysis, while the Phase II was
341 precluded from the analysis as it was affected by the local emission that was disregarded
342 in the model base case. Fig. 5 displays the average RIRs of H_2O_2 , MHP and PAA for



343 alkane, alkene, aromatic and NO_x classes as well as seven most important individual
344 VOC precursors. The results demonstrate that the formation of H₂O₂ was sensitive to
345 alkenes and insensitive to alkanes, aromatics and NO_x. The production of MHP and
346 PAA shows strong dependence of alkenes and NO_x, while it is relatively independent
347 of aromatics and alkanes other than methane. In terms of VOC species with relatively
348 high RIR that is more than 0.001 for H₂O₂ as well as more than 0.01 for MHP and PAA,
349 it is seen that isoprene from the local biogenic emission and trans-2-butene from the
350 anthropogenic emission turn out to be the key VOC species controlling the formation
351 of atmospheric peroxides. Besides, cis-2-butene, cis-2-pentene, propene and 1,2,4-
352 trimethylbenzene also seem to be the major individual VOC precursors as evidence by
353 Fig. 5. Methane is noticed to be an important contributor to the formation of MHP. Such
354 list of VOC species is not consistent with our previous studies over urban Beijing that
355 suggested aromatics (i.e., toluene and dialkylbenzenes) as the dominant VOC precursor
356 of atmospheric peroxides (Zhang et al., 2010; Liang et al., 2013b). It reflects that the
357 relative significance of individual VOC precursors varies from place to place. The
358 distinction between two sites is attributable to the relatively more abundant isoprene,
359 anthropogenic alkenes and much less reactive aromatics at the rural site in the NCP
360 than those at the urban site, Beijing. With the support on the basis of the identification
361 of a small class of key VOC precursors contributing to the formation of peroxides in
362 the atmosphere of NCP, the effective control strategies for mitigating the pollution
363 resulted from atmospheric peroxides can be formulated. In the NCP, it has been
364 revealed that the vehicular exhaust is the predominant source for the responsible VOC
365 species such as propene, trans/cis-2-butenes and trimethylbenzenes in the surrounding
366 areas of the observation site (Yuan et al., 2009; Ran et al., 2011; Li et al., 2014b; Li et
367 al., 2015; Wu et al., 2016), while the vegetation governs the release of isoprene. Taking
368 into account the fact that biogenic emissions of isoprene are not controllable, it is
369 recommended to take measures for vehicle emission reduction in order to mitigate the
370 pollution of atmospheric peroxides in the NCP and hence alleviate their potential
371 harmful effects on air quality, human health and ecosystem.



372 3.3 Direct production of peroxides from biomass burning

373 In the Phase II, the levels of H₂O₂, MHP and PAA were highly elevated in comparison
374 with the other phases, which could not be explained by the photochemical process in
375 the model base case alone. It provides us a hint that an additional formation pathway is
376 required to improve the results of model simulation. In Sect. 3.2, we hypothesized that
377 the direct production of peroxides from biomass burning should serve as an essential
378 source for the unexpected burst of atmospheric peroxides. Here, we tested the
379 hypothesis by means of the box model and linear regression with the observation data
380 from three events mentioned below during the Phase II. It is well known that CO and
381 K⁺ can be used as the reference for the biomass combustion (Koppmann et al., 2005;
382 Reid et al., 2005; Li et al., 2007; Sullivan et al., 2008; Cheng et al., 2013, 2014; Li et
383 al., 2014a; Wang et al., 2015). The averaged CO levels were 0.42±0.16 ppmv,
384 0.79±0.20 ppmv and 0.61±0.20 ppmv for the Phase I, Phase II and Phase III,
385 respectively. The mean K⁺ concentrations were about 0.64±1.19 μg m⁻³ for the Phase
386 I, 2.51±1.53 μg m⁻³ for the Phase II and 0.26±0.21 μg m⁻³ for the Phase III. The
387 abundance of CO and K⁺ during the Phase II increased apparently compared with that
388 during the Phase I and Phase III, which was consistent with the observed intensive
389 biomass burning activities at Wangdu site (Ye, 2015). Nevertheless, in addition to the
390 biomass burning, CO level in the NCP was also affected by anthropogenic activities
391 with the regional transport of polluted air masses, for example, the urban plumes. It has
392 been proved that airborne K⁺ is acceptable as the tracer for biomass burning during
393 summertime in the NCP (Cheng et al., 2013; Wang et al., 2015). Therefore, K⁺ might
394 be a better indicator of biomass burning than CO here. In the Phase II, we identified
395 several biomass burning events with the concentration of K⁺ twice more than the mean
396 value of that in the Phase I and Phase III. Considering the availability of the observation
397 data for atmospheric peroxides, we focused our analysis on three events as follows:
398 Event I (17:00–20:00 on 15 June), Event II (22:00 on 16 June–1:00 on 17 June) and
399 Event III (12:00–15:00 on 17 June) with the duration of over 3 hours.

400 As illustrated in Fig. 3, the model base case cannot reproduce the measurements for



401 atmospheric peroxides in the three events. To match the observation, the primary
402 sources for H₂O₂, MHP and PAA were applied to our model. The strengths of the
403 primary sources were calculated to be about 0.25–0.98 ppbv h⁻¹, 0.09–0.44 ppbv h⁻¹
404 and 0.02–0.14 ppbv h⁻¹ for H₂O₂, MHP and PAA, respectively. These values were on
405 the order of the known secondary production rates of atmospheric peroxides during the
406 three events. It should be pointed out that the estimation was associated with large
407 uncertainties since it did not include the heterogeneous uptake of peroxides by aerosols
408 in the model here. In view of the possible additional sink for atmospheric peroxides as
409 discussed in Sect. 3.4 below, the primary sources for H₂O₂, MHP and PAA might
410 represent the lower limit. The effect of biomass burning on the levels of atmospheric
411 peroxides might be underestimated as well. We underscore that there might exist even
412 larger missing sources for H₂O₂, MHP and PAA due to the scarcity of some important
413 removal pathways of atmospheric peroxides in the model in this section.

414 The results of linear regression involving correlation coefficients and their statistical
415 significance of H₂O₂, MHP and PAA to CO and K⁺ were listed in Table 3 for the three
416 biomass burning events. The relationships between atmospheric peroxides and biomass
417 burning indicators were analyzed separately for each event owing to the variability of
418 fire emissions. A notable trend between atmospheric peroxides and K⁺ was found with
419 correlation coefficients exceeding over the significance threshold, which provided a
420 convincing evidence for the direct production of peroxides from biomass burning as the
421 additional source. Moreover, it was noticed that CO coincided well with K⁺ for the
422 Event I and Event II, exhibiting excellent correlation with atmospheric peroxides (Table
423 3). The enhancement ratios relative of H₂O₂, MHP and PAA to CO were calculated to
424 be at the magnitude ranging from 10⁻³ to 10⁻², which were similar to the enhancement
425 signals of atmospheric peroxides to CO obtained near biomass fires from flights
426 published by Lee et al. (1997).

427 It is noteworthy that several other chemical processes, for example, secondary
428 formation via the photooxidation of potential unmeasured short-lived VOC species
429 emitted from biomass fires prior to our sampling of the plume at the observational site
430 seem to be the alternatives to the direct production from biomass burning as the missing



431 source of atmospheric peroxides in the model. Thus, it appears necessary and desirable
432 to further distinguish the extent to which atmospheric peroxides are generated via the
433 direct production or secondary formation from biomass burning in future research.
434 Laboratory studies are required to simulate the biomass fires in the NCP using
435 combustion chamber to critically characterize the emission factors of atmospheric
436 peroxides to CO and determine their generation mechanisms. Also, more reliable
437 aircraft and ground-based field measurements for the variation of atmospheric
438 peroxides during the harvest seasons in China need to be carried out and would be
439 beneficial to shed some light on the role of biomass burning in the abundance of
440 peroxides in the atmosphere.

441 **3.4 Heterogeneous uptake of peroxides by aerosol**

442 In Sect. 3.2, heterogeneous uptake on atmospheric particles was considered as a suitable
443 explanation for the missing sink for H₂O₂, MHP and PAA during the Phase I and Phase
444 III in view of substantial aerosol loading in the NCP that provided considerably sites
445 for heterogeneous reactions. Here, we made an attempt to implement a parameterization
446 of heterogeneous uptake by aerosols in our box model to resolve the deviation between
447 the simulated and observed data (See Sect. 2.3). Using the uptake coefficient of 1×10^{-3}
448 for H₂O₂, MHP and PAA, a good agreement between the modelled and measured
449 temporal variation of atmospheric peroxides can be obtained in Phase I and Phase III
450 by taking into account the combined model-measurement error that is conservatively
451 assumed to be ~50% (Fig. 3). The calculated H₂O₂, MHP and PAA with the coupling
452 of heterogeneous reaction was on average decreased by about 75% compared to the
453 results in the model base case during the Phase III. The uptake coefficient of 1×10^{-3}
454 approached the upper limit of the laboratory measured value for H₂O₂ on mineral dust
455 (9×10^{-4}) reported by Pradhan et al. (2010), but a little higher than the previous
456 measured values on ambient PM_{2.5} of $(1-5) \times 10^{-4}$ during the summertime over urban
457 Beijing (Wu et al., 2015). It is reasonable as Wu et al. (2015) pointed out that the uptake
458 coefficients for H₂O₂ and organic peroxides on ambient PM_{2.5} are in the same range
459 and show no obvious differences between daytime and nighttime or between non-hazy



460 and hazy conditions.

461 With the adoption of heterogeneous uptake coefficients of 1×10^{-3} , we evaluated the
462 sinks of atmospheric peroxides in the Phase I and Phase III that represented non-haze
463 and haze conditions, respectively. The mean surface area concentration that was
464 corrected for the hygroscopic growth of aerosol was measured to be $968 \mu\text{m}^2 \text{cm}^{-3}$ for
465 Phase I and $1491 \mu\text{m}^2 \text{cm}^{-3}$ for Phase III. Fig. 6 demonstrated that the destruction of
466 atmospheric peroxides during the two phases originated from a diversity of sinks,
467 including photolysis, OH-initiated reaction, dry deposition and heterogeneous uptake.
468 It has been reported that heterogeneous reaction is the most important sink for H_2O_2 in
469 urban (Liang et al., 2013b) and suburban areas (Guo et al., 2014). In contrast, OH-
470 initiated reaction and dry deposition were regarded as the major removal pathways of
471 organic peroxides in rural (Zhang et al., 2012) and forests areas (Nguyen et al., 2015).
472 Here, heterogeneous uptake by aerosols turned out to be the predominant sink for
473 atmospheric peroxides in the NCP, accounting for more than 60% of the total loss,
474 while dry deposition became the marginal removal pathway that contributed $\sim 10\%$ to
475 the destruction of H_2O_2 , MHP and PAA. The role of OH-initiated reaction in the total
476 loss varied between the speciated peroxides with no more than 30%. Photolysis only
477 represented a minor contribution ($< 3\%$). The most prominent feature on haze days was
478 the larger loss of atmospheric peroxides via heterogeneous process, demonstrating the
479 enhanced impact of aerosols on the sink of peroxides during the haze episode compared
480 to that during the non-haze episode. On the basis of the analysis above, we investigated
481 the atmospheric lifetime of peroxides in the NCP with the integration of observation
482 and modelling. The lifetime of H_2O_2 , MHP and PAA were estimated with the
483 concentration-to-time curves between 18:00 and 24:00 LT as the formation of
484 atmospheric peroxides was weak and negligible during this phase. The average lifetime
485 obtained from the field observation between 18:00 and 24:00 LT in the Phase I was
486 around 4.0 h, 5.6 h and 3.1 h for H_2O_2 , MHP and PAA, respectively, which was similar
487 to the values of 3.4 h, 4.3 h and 5.2 h for H_2O_2 , MHP and PAA, respectively, given by
488 our modeling simulation. The lifetime of atmospheric peroxides in the Phase III was



489 ~40% smaller than that in the Phase I. Using the box model, the atmospheric lifetime
490 of H₂O₂, MHP and PAA during the whole Phase I and Phase III was calculated to be
491 about 2.1 h, 2.3 h and 3.0 h, respectively. This is comparable to the literature results
492 with the inclusion of heterogeneous reaction (Liang et al., 2013b; Wu et al., 2015), but
493 notably shorter than the recent studies conducted by Khan et al. (2015) and Nguyen et
494 al. (2015) without the coupling of the heterogeneous process. The simulated lifetime of
495 atmospheric peroxides can be over 10 h by supposing that the loss of H₂O₂, MHP and
496 PAA is merely due to photolysis, OH-initiated reaction and dry deposition. It
497 emphasizes that heterogeneous uptake on aerosols determines the atmospheric lifetime
498 of peroxides.

499 It is worth noting that the heterogeneous uptake of peroxides by aerosols in the
500 atmospheric chemical model is still controversial as it is possibly that the aerosol uptake
501 of HO₂ radicals is the explanation for the missing sink. This raises an interesting
502 question of whether HO₂ uptake or peroxide uptake is responsible for the imbalance
503 between observation and modelling. It has been referred by formerly published
504 literature that aerosol uptake of HO₂ radicals is the major reason for the overprediction
505 of the levels of atmospheric peroxides in the model (de Reus et al., 2005; Mao et al.,
506 2013; Guo et al., 2014). Nevertheless, it is apparent that the extent of HO₂
507 heterogeneous degradation depends on the atmospheric environment, especially the
508 concentration and property of aerosol particles that are various under different
509 conditions. The measured and modelled HO₂ concentrations at Wangdu site are close
510 to each other, implying that the budget of HO₂ is well captured by the box model merely
511 with the gas-phase regional atmospheric chemical mechanism (RACM) comprised (K.
512 Lu, personal communication, 2015). Hence, aerosol uptake of HO₂ radicals is
513 insignificant during Wangdu Campaign 2014 and not taken into account in our model,
514 while heterogeneous uptake of atmospheric peroxides by aerosols is exclusively
515 adopted to improve the reproduction of the observation in the two phases above. It has
516 been inferred that heterogeneous uptake of peroxides on ambient PM_{2.5} is probably
517 resulted from solid surface reactions and aerosol aqueous reactions (Wu et al., 2015),



518 for instance, “Fenton-like” reaction between peroxides and transition metal ions, which
519 is supported by the laboratory studies (Chevallier et al., 2004; Deguillaume et al., 2005)
520 and field observation (Liang et al., 2013b; Guo et al., 2014). Nevertheless, the detailed
521 heterogeneous mechanism containing individual reaction channels was not included in
522 the present work owing to the chemical complexity of the ambient aerosol. Given the
523 potential importance of atmospheric peroxide compounds on the generation of HO_x
524 radicals and aerosol ROS, the aging of mineral dust and SOA and the formation of haze
525 (Huang et al., 2015; Pöschl and Shiraiwa, 2015; Zhang et al., 2015; Li et al., 2016),
526 more comprehensive investigations including laboratory, field and modelling studies
527 on the heterogeneous uptake processes of H₂O₂, MHP, PAA and other peroxides are
528 indispensable to provide concrete evidence to elucidate the chemical budget of
529 atmospheric peroxides in the future.

530 **4 Conclusions**

531 Atmospheric peroxides including H₂O₂, MHP and PAA were measured at a rural site
532 during Wangdu Campaign 2014. The maximum H₂O₂ concentration was observed to
533 be 11.3 ppbv, which was the highest value compared with previous observations in
534 China. The concentrations of atmospheric peroxides were highly elevated during the
535 biomass burning activities, but underwent substantial decline during the haze events.
536 With the application of observation-based model combining measured meteorological
537 parameters and trace gases, we analyzed the chemical budget of peroxides under
538 biomass burning, non-haze and haze conditions. Photochemical formation of
539 atmospheric peroxides was attributed to a small class of alkenes, while it was
540 insensitive to alkanes and aromatics. The key VOC precursors controlling the formation
541 of peroxide compounds were identified to be isoprene, trans/cis-2-butenes, cis-2-
542 pentene, propene and trimethylbenzene. The base model simulation (MCMv3.3.1)
543 underpredicted the levels of atmospheric peroxides up to a factor of 7 during biomass
544 burning events compared with the measurement. The direct production from biomass
545 burning was regarded as the explanation for the unexpected burst of peroxides. To
546 improve the simulated concentrations, the strengths of the primary emissions from



547 biomass burning should be on the same order of the known secondary production rates
548 of atmospheric peroxides. Moreover, the model base case also overpredicted the
549 concentrations of atmospheric peroxides on haze days in comparison with the
550 observation. The heterogeneous uptake by aerosols was suggested to be responsible for
551 the attenuation of peroxides. The model could reproduce the observed values with the
552 introduction of heterogeneous process using the uptake coefficient of 1×10^{-3} for
553 atmospheric peroxides. According to the closure between observed and calculated
554 concentrations, the heterogeneous uptake on aerosol particles was found to be the
555 predominant sink for atmospheric peroxides, accounting for more than 60% of the total
556 loss, followed by the OH-initiated reaction (<30%) and dry deposition (~10%). The
557 mean atmospheric lifetime of peroxides in summer in the NCP was estimated to be
558 around several hours that was in good agreement with previous laboratory studies for
559 the aerosol uptake of peroxides, indicating that heterogeneous reaction determines the
560 atmospheric lifetime of peroxides. In view of the importance of peroxides in
561 tropospheric oxidation capacity and formation potential of secondary aerosols, more
562 reliable investigations focused on the biomass burning emission factors and detailed
563 heterogeneous mechanism of speciated peroxides are urgently required to further
564 quantitatively evaluate the role of biomass burning and heterogeneous uptake in the
565 abundance as well as budget of atmospheric peroxides and facilitate our knowledge of
566 the formation of haze pollution.

567 *Acknowledgements.* This work was funded by the National Natural Science Foundation
568 of China (grants 41275125, 21190051, 21190053, 21477002, and 41421064). The
569 authors would like to thank Min Shao group (Peking University) for their VOCs data
570 and Alfred Wiedensohler group (Leibniz Institute for Tropospheric Research) for their
571 particle surface area concentrations data. The authors wish to gratefully thank the entire
572 Wangdu Campaign 2014 team for the support and collaboration at Wangdu site.

573 **References**

574 Atkinson, R., Baulch, D. L., Cox, R. A., Crowley, J. N., Hampson, R. F., Hynes, R. G.,
575 Jenkin, M. E., Rossi, M. J., Troe, J., and Subcommittee, I.: Evaluated kinetic and



- 576 photochemical data for atmospheric chemistry: Volume II—gas phase reactions of
577 organic species, *Atmos. Chem. Phys.*, 6, 3625–4055, 2006.
- 578 Ayres, J. G., Borm, P., Cassee, F. R., Castranova, V., Donaldson, K., Ghio, A., Harrison,
579 R. M., Hider, R., Kelly, F., Kooter, I. M., Maranok, F., Maynardl, R. L., Mudwaym,
580 I., Nel, A., Sioutaso, C., Smithp, S., Baeza-Squibank, A., Chon, A., Dugganq S., and
581 Froinesn J.: Evaluating the toxicity of airborne particulate matter and nanoparticles
582 by measuring oxidative stress potential—a workshop report and consensus statement,
583 *Inhal. Toxicol.*, 20, 75–99, 2008.
- 584 Bohn, B., Corlett, G. K., Gillmann, M., Sanghavi, S., Stange, G., Tensing, E.,
585 Vrekoussis, M., Bloss, W. J., Clapp, L. J., Kortner, M., Dorn, H.P., Monks, P. S.,
586 Platt, U., Plass-Dulmer, C., Mihalopoulos, N., Heard, D. E., Clemitshaw, K. C.,
587 Meixner, F. X., Prevot, A. S. H., and Schmitt, R.: Photolysis frequency measurement
588 techniques: results of a comparison within the ACCENT project, *Atmos. Chem.*
589 *Phys.*, 8, 5373–5391, 2008.
- 590 Bossolasco, A., Faragó, E. P., Schoemaeker, C., and Fittschen, C.: Rate constant of the
591 reaction between CH_3O_2 and OH radicals, *Chem. Phys. Lett.*, 593, 7–13, 2014.
- 592 Calvert, J. G., Lazrus, A., Kok, G. L., Heikes, B. G., Walega, J. G., Lind, J., and Cantrell,
593 C. A.: Chemical mechanisms of acid generation in the troposphere, *Nature*, 317,
594 27–35, 1985.
- 595 Cardelino, C. A., and Chameides, W. L.: An observation-based model for analyzing
596 ozone precursor relationships in the urban atmosphere, *J. Air Waste Manage. Assoc.*,
597 45, 161–180, 1995.
- 598 Chao, W., Hsieh, J. T., and Chang, C. H.: Direct kinetic measurement of the reaction of
599 the simplest Criegee intermediate with water vapor, *Science*, 347, 751–754, 2015.
- 600 Chen, X., Aoki, M., Takami, A., Chai, F., and Hatakeyama, S.: Effect of ambient-level
601 gas-phase peroxides on foliar injury, growth, and net photosynthesis in Japanese
602 radish (*Raphanus sativus*), *Environ. Pollut.*, 158, 1675–1679, 2010.
- 603 Chen, Z. M., Wang, H. L., Zhu, L. H., Wang, C. X., Jie, C. Y., and Hua, W.: Aqueous-
604 phase ozonolysis of methacrolein and methyl vinyl ketone: a potentially important
605 source of atmospheric aqueous oxidants, *Atmos. Chem. Phys.*, 8, 2255–2265, 2008.



- 606 Cheng, Y., Engling, G., He, K. B., Duan, F. K., Ma, Y. L., Du, Z. Y., Liu, J. M., Zheng,
607 M., and Weber, R. J.: Biomass burning contribution to Beijing aerosol, Atmos. Chem.
608 Phys., 13, 7765–7781, 2013.
- 609 Cheng, Y., Engling, G., He, K. B., Duan, F. K., Du, Z. Y., Ma, Y. L., Liang, L. L., Lu,
610 Z. F., Liu, J. M., Zheng, M., and Weber, R. J.: The characteristics of Beijing aerosol
611 during two distinct episodes: Impacts of biomass burning and fireworks, Environ.
612 Pollut., 185, 149–157, 2014.
- 613 Chevallier, E., Jolibois, R. D., Meunier, N., Carlier, P., and Monod, A.: “Fenton-like”
614 reactions of methylhydroperoxide and ethylhydroperoxide with Fe²⁺ in liquid
615 aerosols under tropospheric conditions, Atmos. Environ., 38, 921–933, 2004.
- 616 de Reus, M., Fischer, H., Sander, R., Gros, V., Kormann, R., Salisburly, G., Van
617 Dingenen, R., Williams, J., Zöllner, M., and Lelieveld, J.: Observations and model
618 calculations of trace gas scavenging in a dense Saharan dust plume during
619 MINATROC, Atmos. Chem. Phys., 5, 1787–1803, 2005.
- 620 Deguillaume, L., Leriche, M., Desboeufs, K., Mailhot, G., George, C., and Chaumerliac,
621 N.: Transition metals in atmospheric liquid phases: sources, reactivity, and sensitive
622 parameters, Chem. Rev., 105, 3388–3431, 2005.
- 623 Draxler, R. R., and Rolph, G. D.: HYSPLIT (HYbrid Single-Particle Lagrangian
624 Integrated Trajectory) model access via NOAA ARL READY website ([http://www.
625 arl.noaa.gov/ready/hysplit4.html](http://www.arl.noaa.gov/ready/hysplit4.html)), NOAA Air Resources Laboratory, Silver Spring,
626 MD, 2012.
- 627 Emmerson, K. M., Carslaw, N., Carslaw, D. C., Lee, J. D., McFiggans, G., Bloss, W. J.,
628 Gravestock, T., Heard, D. E., Hopkins, J., Ingham, T., Pilling, M. J., Smith, S. C.,
629 Jacob, M., and Monks, P. S.: Free radical modelling studies during the UK TORCH
630 Campaign in Summer 2003, Atmos. Chem. Phys., 7, 167–181, 2007.
- 631 Epstein, S. A., Blair, S. L., and Nizkorodov, S. A.: Direct photolysis of α -pinene
632 ozonolysis secondary organic aerosol: effect on particle mass and peroxide content,
633 Environ. Sci. Technol., 48, 11251–11258, 2014.
- 634 Ervens, B., George, C., Williams, J. E., Buxton, G. V., Salmon, G. A., Bydder, M.,
635 Wilkinson, F., Dentener, F., Mirabel, P., Wolke, R. and Herrmann, H.: CAPRAM 2.



- 636 4 (MODAC mechanism): an extended and condensed tropospheric aqueous phase
637 mechanism and its application, *J. Geophys. Res.*, 108, 4426, 2003.
- 638 Fischer, H., Pozzer, A., Schmitt, T., Jöckel, P., Klippel, T., Taraborrelli, D., and
639 Lelieveld, J.: Hydrogen peroxide in the marine boundary layer over the South
640 Atlantic during the OOMPH cruise in March 2007, *Atmos. Chem. Phys.*, 15,
641 6971–6980, 2015.
- 642 Fittschen, C., Whalley, L. K., and Heard, D. E.: The reaction of CH_3O_2 radicals with
643 OH radicals: a neglected sink for CH_3O_2 in the remote atmosphere, *Environ. Sci.*
644 *Technol.*, 48, 7700–7701, 2014.
- 645 Guo, J., Tilgner, A., Yeung, C., Wang, Z., Louie, P. K. K., Luk, C. W. Y., Xu, Z., Yuan,
646 C., Gao, Y., Poon, S., Herrmann, H., Lee, S., Lam, K. S. and Wang, T.: Atmospheric
647 peroxides in a polluted subtropical environment: seasonal variation, sources and
648 sinks, and importance of heterogeneous processes, *Environ. Sci. Technol.*, 48,
649 1443–1450, 2014.
- 650 He, S. Z., Chen, Z. M., Zhang, X., Zhao, Y., Huang, D. M., Zhao, J. N., Zhu, T., Hu,
651 M., and Zeng, L. M.: Measurement of atmospheric hydrogen peroxide and organic
652 peroxides in Beijing before and during the 2008 Olympic Games: chemical and
653 physical factors influencing their concentrations, *J. Geophys. Res.*, 115, D17307,
654 2010.
- 655 Hellpointner, E., and Gäb, S.: Detection of methyl, hydroxymethyl and hydroxyethyl
656 hydroperoxides in air and precipitation, *Nature*, 631–634, 1989.
- 657 Hewitt, C. N., and Kok, G. L.: Formation and occurrence of organic hydroperoxides in
658 the troposphere: laboratory and field observations, *J. Atmos. Chem.*, 12, 181–194,
659 1991.
- 660 Hofzumahaus, A., Rohrer, F., Lu, K., Bohn, B., Brauers, T., Chang, C. C., Fuchs, H.,
661 Holland, F., Kita, K., Kondo, Y., Li, X., Lou, S., Shao, M., Zeng, L., Wahner, A. and
662 Zhang, Y.: Amplified trace gas removal in the troposphere, *Science*, 324, 1702–1704,
663 2009.
- 664 Hua, W., Chen, Z. M., Jie, C. Y., Kondo, Y., Hofzumahaus, A., Takegawa, N., Chang,
665 C. C., Lu, K. D., Miyazaki, Y., Kita, K., Wang, H. L., Zhang Y. H., and Hu, M.:



- 666 Atmospheric hydrogen peroxide and organic hydroperoxides during PRIDE-PRD'06,
667 China: their concentration, formation mechanism and contribution to secondary
668 aerosols, *Atmos. Chem. Phys.*, 8, 6755–6773, 2008.
- 669 Huang, D., Chen, Z. M., Zhao, Y., and Liang, H.: Newly observed peroxides and the
670 water effect on the formation and removal of hydroxyalkyl hydroperoxides in the
671 ozonolysis of isoprene, *Atmos. Chem. Phys.*, 13, 5671–5683, 2013.
- 672 Huang, L. B., Zhao, Y., Li, H., and Chen, Z. M. Kinetics of heterogeneous reaction of
673 sulfur dioxide on authentic mineral dust: effects of relative humidity and hydrogen
674 peroxide, *Environ. Sci. Technol.*, 49, 10797–10805, 2015.
- 675 Huang, R. J., Zhang, Y. L., Bozzetti, C., Ho, K. F., Cao, J. J., Han, Y. M., Daellenbach,
676 K. R., Slowik, J. G., Platt, S. M., Canonaco, F., Zotter, P., Wolf, R., Pieber, S. M.,
677 Bruns, E. A., Crippa, M., Ciarelli, G., Piazzalunga, A., Schwikowski, M., Abbaszade,
678 G., Schnelle-Kreis, J., Zimmermann, R., An, Z., Szidat, S., Baltensperger, U.,
679 Haddad, I. E., and Prévôt A. S. H.: High secondary aerosol contribution to particulate
680 pollution during haze events in China, *Nature*, 514, 218–222, 2014.
- 681 Jacob, D. J.: Heterogeneous chemistry and tropospheric ozone, *Atmos. Environ.*, 34,
682 2131–2159, 2000.
- 683 Jenkin, M. E., Saunders, S. M., Pilling, M. J.: The tropospheric degradation of volatile
684 organic compounds: a protocol for mechanism development, *Atmos. Environ.*, 31,
685 81–104, 1997.
- 686 Jenkin, M. E., Saunders, S. M., Wagner, V., and Pilling, M. J.: Protocol for the
687 development of the Master Chemical Mechanism, MCM v3 (Part B): tropospheric
688 degradation of aromatic volatile organic compounds, *Atmos. Chem. Phys.*, 3,
689 181–193, 2003.
- 690 Jenkin, M. E., Young, J. C., and Rickard, A. R.: The MCM v3. 3. 1 degradation scheme
691 for isoprene, *Atmos. Chem. Phys.*, 15, 11433–11459, 2015.
- 692 Khan, M. A. H., Cooke, M. C., Utembe, S. R., Xiao, P., Morris, W. C., Derwent, R. G.,
693 Archibald, A. T., Jenkin, M. E., Percival, C. J., and Shallcross, D. E.: The global
694 budgets of organic hydroperoxides for present and pre-industrial scenarios, *Atmos.*
695 *Environ.*, 110, 65–74, 2015.



- 696 Koppmann, R., Czapiewski, K. V., and Reid, J. S.: A review of biomass burning
697 emissions, part I: gaseous emissions of carbon monoxide, methane, volatile organic
698 compounds, and nitrogen containing compounds, Atmos. Chem. Phys. Discuss., 5,
699 10455–10516, 2005.
- 700 Kroll, J. H., and Seinfeld, J. H.: Chemistry of secondary organic aerosol: Formation and
701 evolution of low-volatility organics in the atmosphere, Atmos. Environ., 42, 3593–
702 3624, 2008.
- 703 Lee, M., Heikes, B. G., Jacob, D. J., Sachse, G., and Anderson, B.: Hydrogen peroxide,
704 organic hydroperoxide, and formaldehyde as primary pollutants from biomass
705 burning, J. Geophys. Res., 102, 1301–1309, 1997.
- 706 Lee, M., Heikes, B. G., and Jacob, D. J.: Enhancements of hydroperoxides and
707 formaldehyde in biomass burning impacted air and their effect on atmospheric
708 oxidant cycles, J. Geophys. Res., 103, 13201–13212, 1998.
- 709 Lee, M., Heikes, B. G., and O'Sullivan, D. W.: Hydrogen peroxide and organic
710 hydroperoxide in the troposphere: a review, Atmos. Environ., 34, 3475–3494, 2000.
- 711 Li, H., Chen, Z. M., Huang, L. B., and Huang, D.: Organic peroxides' gas-particle
712 partitioning and rapid heterogeneous decomposition on secondary organic aerosol,
713 Atmos. Chem. Phys., 16, 1837–1848, 2016.
- 714 Li, J., Song, Y., Mao, Y., Mao, Z., Wu, Y., Li, M., Huang, X., He, Q., and Hu, M.:
715 Chemical characteristics and source apportionment of PM_{2.5} during the harvest
716 season in eastern China's agricultural regions, Atmos. Environ., 92, 442–448, 2014a.
- 717 Li, L., Xie, S., Zeng, L., Wu, R., and Li, J.: Characteristics of volatile organic
718 compounds and their role in ground-level ozone formation in the Beijing-Tianjin-
719 Hebei region, China, Atmos. Environ., 113, 247–254, 2015.
- 720 Li, M., Zhang, Q., Streets, D. G., He, K. B., Cheng, Y. F., Emmons, L. K., Huo, H.,
721 Kang, S. C., Lu, Z., Shao, M., Su, H., Yu, X., Zhang, Y.: Mapping Asian
722 anthropogenic emissions of non-methane volatile organic compounds to multiple
723 chemical mechanisms, Atmos. Chem. Phys., 14, 5617–5638, 2014b.
- 724 Li, X., Wang, S., Duan, L., Hao, J., Li, C., Chen, Y., and Yang, L.: Particulate and trace
725 gas emissions from open burning of wheat straw and corn stover in China, Environ.



- 726 Sci. Technol., 41, 6052–6058, 2007.
- 727 Li, X., Rohrer, F., Brauers, T., Hofzumahaus, A., Lu, K., Shao, M., Zhang, Y. H., and
728 Wahner, A.: Modeling of HCHO and CHOCHO at a semi-rural site in southern
729 China during the PRIDE-PRD2006 campaign, Atmos. Chem. Phys., 14,
730 12291–12305, 2014c.
- 731 Liang, H., Chen, Z., Wu, Q., Huang, D., and Zhao, Y.: Do aerosols influence the diurnal
732 variation of H₂O₂ in the atmosphere?, AGU Fall Meeting Abstracts, 2013a.
- 733 Liang, H., Chen, Z. M., Huang, D., Zhao, Y., and Li, Z. Y.: Impacts of aerosols on the
734 chemistry of atmospheric trace gases: a case study of peroxides and HO₂ radicals,
735 Atmos. Chem. Phys., 13, 11259–11276, 2013b.
- 736 Liu, H. J.: Measurement of aerosol light scattering enhancement factor and study on
737 hygroscopicity parameter, Ph. D, thesis, Peking University, China, 2015.
- 738 Liu, Y., Yuan, B., Li, X., Shao, M., Lu, S. H., Li, Y., Chang, C. C., Wang, Z., Hu, W.,
739 Huang, X., He, L., Zeng, L., Hu, M., and Zhu, T.: Impact of pollution controls in
740 Beijing on atmospheric oxygenated volatile organic compounds (OVOCs) during
741 the 2008 Olympic Games: observation and modeling implications, Atmos. Chem.
742 Phys., 15, 3045–3062, 2015.
- 743 Liu, Y., Lu, K., Dong, H., Li, X., Cheng, P., Zou, Q., Wu, Y., Liu, X., and Zhang, Y.: In
744 situ monitoring of atmospheric nitrous acid based on multi-pumping flow system
745 and liquid waveguide capillary cell, J. Environ. Sci., 2016, in press.
- 746 Lu, K. D., Rohrer, F., Holland, F., Fuchs, H., Bohn, B., Brauers, T., Chang, C. C.,
747 Haeseler, R., Hu, M., Kita, K., Kondo, Y., Li, X., Lou, S. R., Nehr, S., Shao, M.,
748 Zeng, L. M., Wahner, A., Zhang, Y. H., and Hofzumahaus, A.: Observation and
749 modelling of OH and HO₂ concentrations in the Pearl River Delta 2006: a missing
750 OH source in a VOC rich atmosphere, Atmos Chem Phys, 12, 1541–1569, 2012.
- 751 Madronich, S.: The Tropospheric visible Ultra-violet (TUV) model web page, available
752 at: <http://www.acd.ucar.edu/TUV>, 2002.
- 753 Mao, J., Jacob, D. J., Evans, M. J., Olson, J. R., Ren, X., Brune, W. H., St Clair, J. M.,
754 Crouse, J. D., Spencer, K. M., Beaver, M. R., Wennberg, P. O., Cubison, M. J.,
755 Jimenez, J. L., Fried, A., Weibring, P., Walega, J. G., Hall, S. R., Weinheimer, A. J.,



- 756 Cohen, R. C., Chen, G., Crawford, J. H., McNaughton, C., Clarke, A. D., Jaeglé, L.,
757 Fisher, J. A., Yantosca, R. M., Le Sager, P., and Carouge, C.: Chemistry of hydrogen
758 oxide radicals (HO_x) in the Arctic troposphere in spring, *Atmos. Chem. Phys.*, 10,
759 5823–5838, 2010.
- 760 Mao, J., Fan, S., Jacob, D. J., and Travis, K. R.: Radical loss in the atmosphere from
761 Cu-Fe redox coupling in aerosols, *Atmos. Chem. Phys.*, 13, 509–519, 2013.
- 762 Neeb, P., Sauer, F., Horie, O., and Moortgat, G. K.: Formation of hydroxymethyl
763 hydroperoxide and formic acid in alkene ozonolysis in the presence of water vapour,
764 *Atmos. Environ.*, 31, 1417–1423, 1997.
- 765 Nguyen, T. B., Crouse, J. D., Teng, A. P., Clair, J. M. S., Paulot, F., Wolfe, G. M., and
766 Wennberg, P. O.: Rapid deposition of oxidized biogenic compounds to a temperate
767 forest, *Proc. Nat. Acad. Sci.*, 112, E392–E401, 2015.
- 768 Pöschl, U., and Shiraiwa, M.: Multiphase chemistry at the atmosphere-biosphere
769 interface influencing climate and public health in the anthropocene, *Chem. Rev.*, 115,
770 4440–4475, 2015.
- 771 Pradhan, M., Kyriakou, G., Archibald, A. T., Papageorgiou, A. C., Kalberer, M., and
772 Lambert, R. M.: Heterogeneous uptake of gaseous hydrogen peroxide by Gobi and
773 Saharan dust aerosols: a potential missing sink for H_2O_2 in the troposphere, *Atmos.*
774 *Chem. Phys.*, 10, 7127–7136, 2010.
- 775 Ran, L., Zhao, C. S., Xu, W. Y., Lu, X. Q., Han, M., Lin, W. L., Yan, P., Xu, X. B., Deng,
776 Z. Z., Ma, N., Liu, P. F., Yu, J., Liang, W. D., and Chen, L. L.: VOC reactivity and
777 its effect on ozone production during the HaChi summer campaign, *Atmos. Chem.*
778 *Phys.*, 11, 4657–4667, 2011.
- 779 Reeves, C. E., and Penkett, S. A.: Measurements of peroxides and what they tell us,
780 *Chem. Rev.*, 103, 5199–5218, 2003.
- 781 Reid, J. S., Koppmann, R., Eck, T. F., and Eleuterio, D. P.: A review of biomass burning
782 emissions part II: intensive physical properties of biomass burning particles, *Atmos.*
783 *Chem. Phys.*, 5, 799–825, 2005.
- 784 Sander, S. P., Abbatt, J., Barker, J. R., Burkholder, J. B., Friedl, R. R., Golden, D. M.,
785 Huie, R. E., Kolb, C. E., Kurylo, M. J., Moortgat, G. K., Orkin, V. L., and Wine, P.



- 786 H.: Chemical kinetics and photochemical data for use in atmospheric studies,
787 Evaluation No, 17, JPL Publication 10–6, Jet Propulsion Laboratory, Pasadena, CA,
788 USA, available at: <http://jpldataeval.jpl.nasa.gov>, 2011.
- 789 Sarwar, G., Godowitch, J., Henderson, B. H., Fahey, K., Pouliot, G., Hutzell, W. T.,
790 Mathur, R., Kang, D., Goliff, W. S., and Stockwell, W. R.: A comparison of
791 atmospheric composition using the Carbon Bond and Regional Atmospheric
792 Chemistry Mechanisms, *Atmos. Chem. Phys.*, 13, 9695–9712, 2013.
- 793 Sauer, F., Beck, J., Schuster, G., and Moortgat, G. K.: Hydrogen peroxide, organic
794 peroxides and organic acids in a forested area during FIELDVOC'94, *Chemosphere*,
795 3, 309–326, 2001.
- 796 Saunders, S. M., Jenkin, M. E., Derwent, R. G., and Pilling, M. J.: Protocol for the
797 development of the Master Chemical Mechanism, MCM v3 (Part A): tropospheric
798 degradation of non-aromatic volatile organic compounds, *Atmos. Chem. Phys.*, 3,
799 161–180, 2003.
- 800 Seinfeld, J. H., and Pandis, S. N.: *Atmospheric Chemistry and Physics: From Air
801 Pollution to Climate Change*, John Wiley & Sons, 2006.
- 802 Stein, A. F., and Saylor, R. D.: Sensitivities of sulfate aerosol formation and oxidation
803 pathways on the chemical mechanism employed in simulations, *Atmos. Chem. Phys.*,
804 12, 8567–8574, 2012.
- 805 Sullivan, A. P., Holden, A. S., Patterson, L. A., McMeeking, G. R., Kreidenweis, S. M.,
806 Malm, W. C., Hao, W. M., Wold, C. E., and Collett, J. L.: A method for smoke marker
807 measurements and its potential application for determining the contribution of
808 biomass burning from wildfires and prescribed fires to ambient PM_{2.5} organic carbon,
809 *J. Geophys. Res.*, 113, D22302, 2008.
- 810 Tao, M., Chen, L., Su, L., and Tao, J.: Satellite observation of regional haze pollution
811 over the North China Plain, *J. Geophys. Res.*, 117, D12203, 2012.
- 812 Wang, H. L., Huang, D., Zhang, X., Zhao, Y., and Chen, Z. M.: Understanding the
813 aqueous phase ozonolysis of isoprene: distinct product distribution and mechanism
814 from the gas phase reaction, *Atmos. Chem. Phys.*, 12, 7187–7198, 2012.
- 815 Wang, L., Xin, J., Li, X., and Wang, Y., The variability of biomass burning and its



- 816 influence on regional aerosol properties during the wheat harvest season in North
817 China, *Atmos. Res.*, 157, 153–163, 2015.
- 818 Wang, M., Zeng, L., Lu, S., Shao, M., Liu, X., Yu, X., Chen, W., Yuan, B., Zhang, Q.,
819 Hu, M., and Zhang, Z.: Development and validation of a cryogen-free automatic gas
820 chromatograph system (GC-MS/FID) for online measurements of volatile organic
821 compounds, *Anal. Methods*, 6, 9424–9434, 2014.
- 822 Winiberg, F. A. F., Dillon, T. J., Orr, S. C., Groß, C. B., Bejan, I., Brumby, C. A., Evans,
823 M. J., Smith, S. C., Heard, D. E., and Seakins, P. W.: Direct measurements of OH
824 and other product yields from the $\text{HO}_2 + \text{CH}_3\text{C}(\text{O})\text{O}_2$ reaction, *Atmos. Chem. Phys.*,
825 16, 4023–4042, 2016.
- 826 Wu, Q. Q., Huang, L. B., Liang, H., Zhao, Y., Huang, D., and Chen, Z. M.:
827 Heterogeneous reaction of peroxyacetic acid and hydrogen peroxide on ambient
828 aerosol particles under dry and humid conditions: kinetics, mechanism and
829 implications, *Atmos. Chem. Phys.*, 15, 6851–6866, 2015.
- 830 Wu, R., Bo, Y., Li, J., Li, L., Li, Y., and Xie, S.: Method to establish the emission
831 inventory of anthropogenic volatile organic compounds in China and its application
832 in the period 2008–2012, *Atmos. Environ.*, 127, 244–254, 2016.
- 833 Ye, N. N.: Observations and budget analysis of ambient nitrous acid (HONO) in
834 Wangdu, a rural site in North China Plain, Master thesis, Peking University, China,
835 2015.
- 836 Yokelson, R. J., Crounse, J. D., DeCarlo, P. F., Karl, T., Urbanski, S., Atlas, E., Campos,
837 T., Shinozuka, Y., Kapustin, V., Clarke, A. D., Weinheimer, A., Knapp, D. J.,
838 Montzka, D. D., Holloway, J., Weibring, P., Flocke, F., Zheng, W., Toohey, D.,
839 Wennberg, P. O., Wiedinmyer, C., Mauldin, L., Fried, A., Richter, D., Walega, J.,
840 Jimenez, J. L., Adachi, K., Buseck, P. R., Hall, S. R., and Shetter, R.: Emissions from
841 biomass burning in the Yucatan, *Atmos. Chem. Phys.*, 9, 5785–5812, 2009.
- 842 Yuan, Z., Lau, A. K. H., Shao, M., Louie, P. K. K., Liu, S. C., and Zhu, T.: Source
843 analysis of volatile organic compounds by positive matrix factorization in urban and
844 rural environments in Beijing, *J. Geophys. Res.*, 114, D00G15, 2009.
- 845 Zhang, L., Brook, J. R., and Vet, R.: A revised parameterization for gaseous dry



- 846 deposition in air-quality models, Atmos. Chem. Phys., 3, 2067–2082, 2003.
- 847 Zhang, R. Y., Wang, G. H., Guo, S., Zamora, M. L., Ying, Q., Lin, Y., Wang, W. G., Hu,
848 M., and Wang, Y.: Formation of urban fine particulate matter, Chem. Rev., 115,
849 3803–3855, 2015.
- 850 Zhang, X., Chen, Z. M., He, S. Z., Hua, W., Zhao, Y., and Li, J. L.: Peroxyacetic acid
851 in urban and rural atmosphere: concentration, feedback on PAN–NO_x cycle and
852 implication on radical chemistry, Atmos. Chem. Phys., 10, 737–748, 2010.
- 853 Zhang, X., He, S. Z., Chen, Z. M., Zhao, Y., and Hua, W.: Methyl hydroperoxide
854 (CH₃OOH) in urban, suburban and rural atmosphere: ambient concentration, budget,
855 and contribution to the atmospheric oxidizing capacity, Atmos. Chem. Phys., 12,
856 8951–8962, 2012.
- 857 Zhao, R., Lee, A. K. Y., Soong, R., Simpson, A. J., and Abbatt, J. P. D.: Formation of
858 aqueous-phase α -hydroxyhydroperoxides (α -HHP): potential atmospheric impacts,
859 Atmos. Chem. Phys., 13, 5857–5872, 2013a.
- 860 Zhao, Y., Chen, Z. M., Shen, X. L., and Huang, D.: Heterogeneous reactions of gaseous
861 hydrogen peroxide on pristine and acidic gas-processed calcium carbonate particles:
862 Effects of relative humidity and surface coverage of coating, Atmos. Environ., 67,
863 63–72, 2013b.
- 864 Ziemann, P. J., and Atkinson, R.: Kinetics, products, and mechanisms of secondary
865 organic aerosol formation, Chem. Soc. Rev., 41, 6582–6605, 2012.



Table 1. Summary of the concentrations of atmospheric peroxides during Wangdu Campaign 2014.

		H ₂ O ₂ (ppbv)	MHP (ppbv)	PAA (ppbv)
24 h	D.L. ^a	0.01	0.01	0.01
	N ^b	1797	1797	1797
	Mean	0.51	0.17	0.04
	S.D. ^c	0.90	0.20	0.11
	Median	0.19	0.11	0.01
	Maximum	11.3	1.25	1.49
Daytime (06:00–18:00 LT ^d)	N ^b	829	829	829
	Mean	0.55	0.16	0.03
	S.D. ^c	0.83	0.17	0.12
	Median	0.24	0.12	0.01
	Maximum	10.20	1.20	1.49
Nighttime (18:00–06:00 LT ^d)	N ^b	968	968	968
	Mean	0.48	0.17	0.04
	S.D. ^c	0.96	0.23	0.11
	Median	0.15	0.11	0.01
	Maximum	11.33	1.25	1.47

^a D.L.: detection limit.

^b N: number of samples.

^c S.D.: standard deviation.

^d LT: local time.



Table 2. Chemical mechanisms for $\text{CH}_3\text{C}(\text{O})\text{O}_2$ and CH_3O_2 related chemistry modified or added to MCMv3.3.1.

Reactions	Rate constants ($\text{cm}^3 \text{ molecule}^{-1} \text{ s}^{-1}$)	Reference
$\text{CH}_3\text{C}(\text{O})\text{O}_2$ chemistry		
$\text{CH}_3\text{C}(\text{O})\text{O}_2 + \text{HO}_2 \rightarrow \text{CH}_3\text{C}(\text{O})\text{OOH} + \text{O}_2$	$2.40 \times 10^{-11} \times 0.37$	Winiberg et al. (2016)
$\text{CH}_3\text{C}(\text{O})\text{O}_2 + \text{HO}_2 \rightarrow \text{CH}_3\text{C}(\text{O})\text{OH} + \text{O}_3$	$2.40 \times 10^{-11} \times 0.12$	Winiberg et al. (2016)
$\text{CH}_3\text{C}(\text{O})\text{O}_2 + \text{HO}_2 \rightarrow \text{CH}_3 + \text{CO}_2 + \text{OH} + \text{O}_2$	$2.40 \times 10^{-11} \times 0.51$	Winiberg et al. (2016)
CH_3O_2 chemistry		
$\text{CH}_3\text{O}_2 + \text{OH} \rightarrow \text{PRODUCT}$	2.80×10^{-10}	Fittschen et al. (2014)



Table 3. Linear regression of atmospheric peroxide species to CO and K⁺ for three biomass burning events during the Phase II (15 June–17 June). Correlation coefficients shown in italic and bold indicate statistical significance ($p < 0.05$) and higher statistical significance ($p < 0.01$), respectively.

Species	Slope ^a	Correlation coefficient		N ^b	Critical correlation coefficient
		CO	K ⁺		
<i>Event I</i>					
H ₂ O ₂	2.17×10^{-3}	0.8144	0.8432	10	0.7646 ($p < 0.01$), 0.6319 ($p < 0.05$)
MHP	1.23×10^{-3}	<i>0.6873</i>	<i>0.7624</i>	10	
PAA	7.16×10^{-4}	0.8378	0.9515	10	
<i>Event II</i>					
H ₂ O ₂	1.32×10^{-2}	0.9134	0.8538	11	0.7348 ($p < 0.01$), 0.6021 ($p < 0.05$)
MHP	2.30×10^{-3}	0.8876	<i>0.7042</i>	11	
PAA	6.73×10^{-4}	0.8399	0.5330	11	
<i>Event III</i>					
H ₂ O ₂	N/A ^c	N/A ^c	0.9632	9	0.7977 ($p < 0.01$), 0.6664 ($p < 0.05$)
MHP	N/A ^c	N/A ^c	0.8741	9	
PAA	N/A ^c	N/A ^c	0.8436	9	

^a Slope: enhancement ratio of speciated peroxides relative to CO.

^b N: number of samples.

^c N/A: missing data.

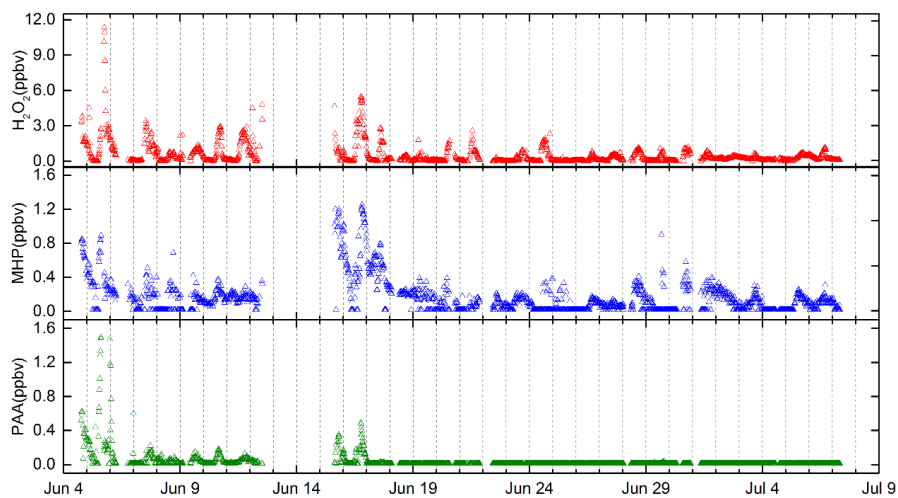


Figure 1. Temporal profile for atmospheric peroxides over the entire Wangdu Campaign 2014.

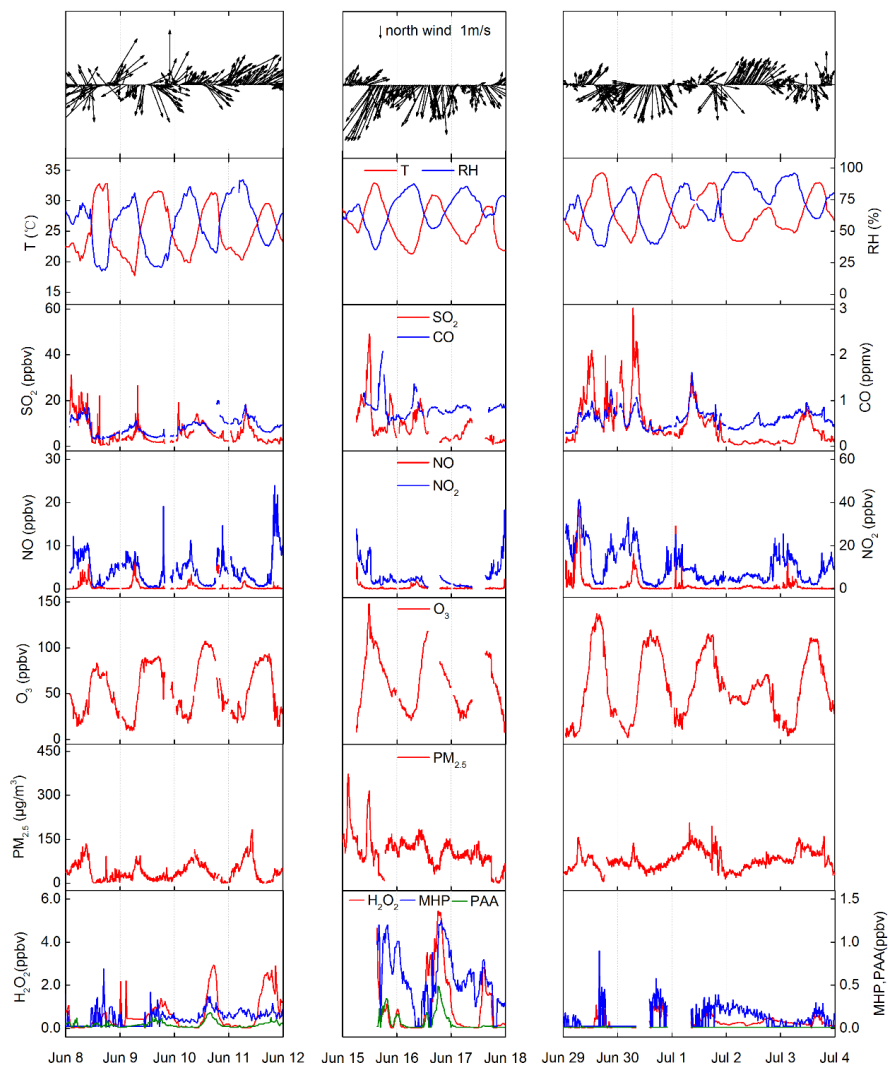


Figure 2. Time series of meteorological parameters, chemical species and atmospheric peroxides for Phase I (8 June–11 June), Phase II (15 June–17 June) and Phase III (29 June–3 July).

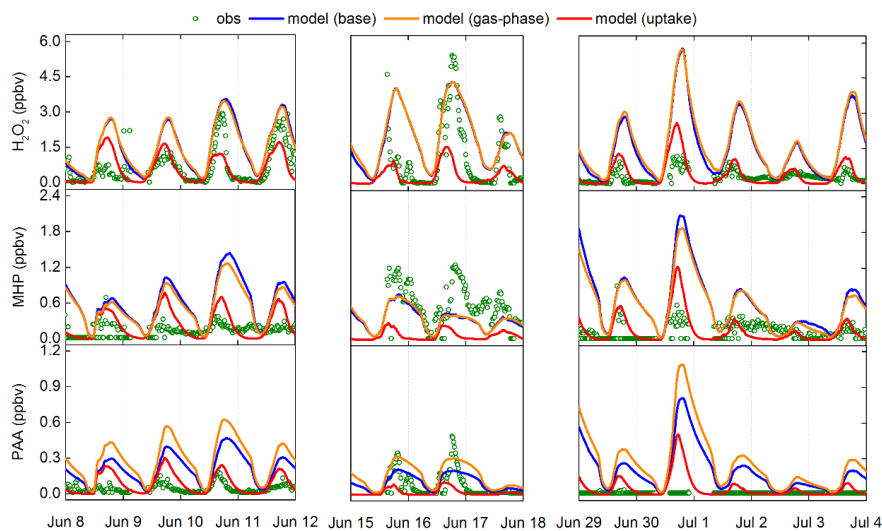


Figure 3. Observed and modelled concentrations of atmospheric peroxides for Phase I (8 June–11 June), Phase II (15 June–17 June) and Phase III (29 June–3 July). The green circles represent observed concentrations. The blue, orange and red lines indicate the modelled concentrations from three different scenarios: base case, new gas-phase reaction case and heterogeneous uptake case, respectively.

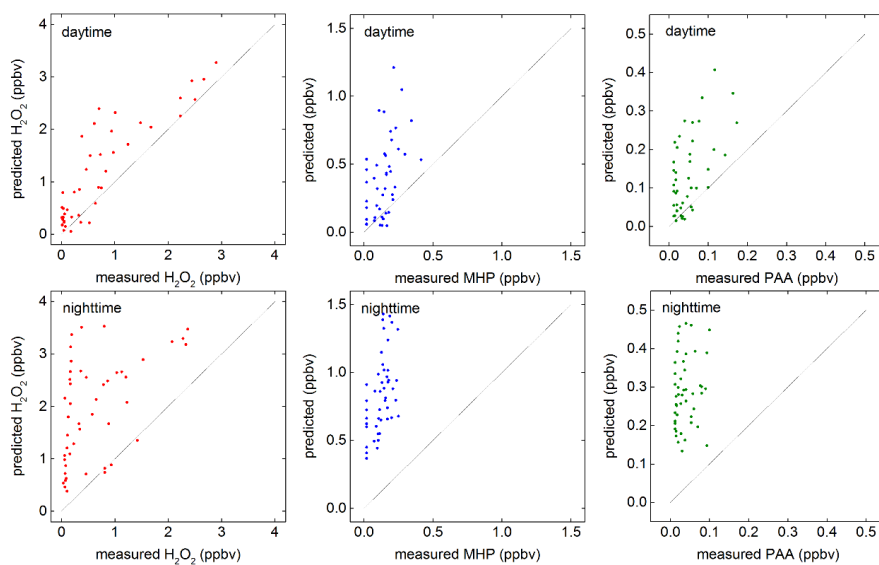


Figure 4. Comparisons between measured and predicted concentrations of atmospheric peroxides for daytime and nighttime during the Phase I (8 June–11 June). The solid lines represent the 1:1 ratio of observed to modelled values.

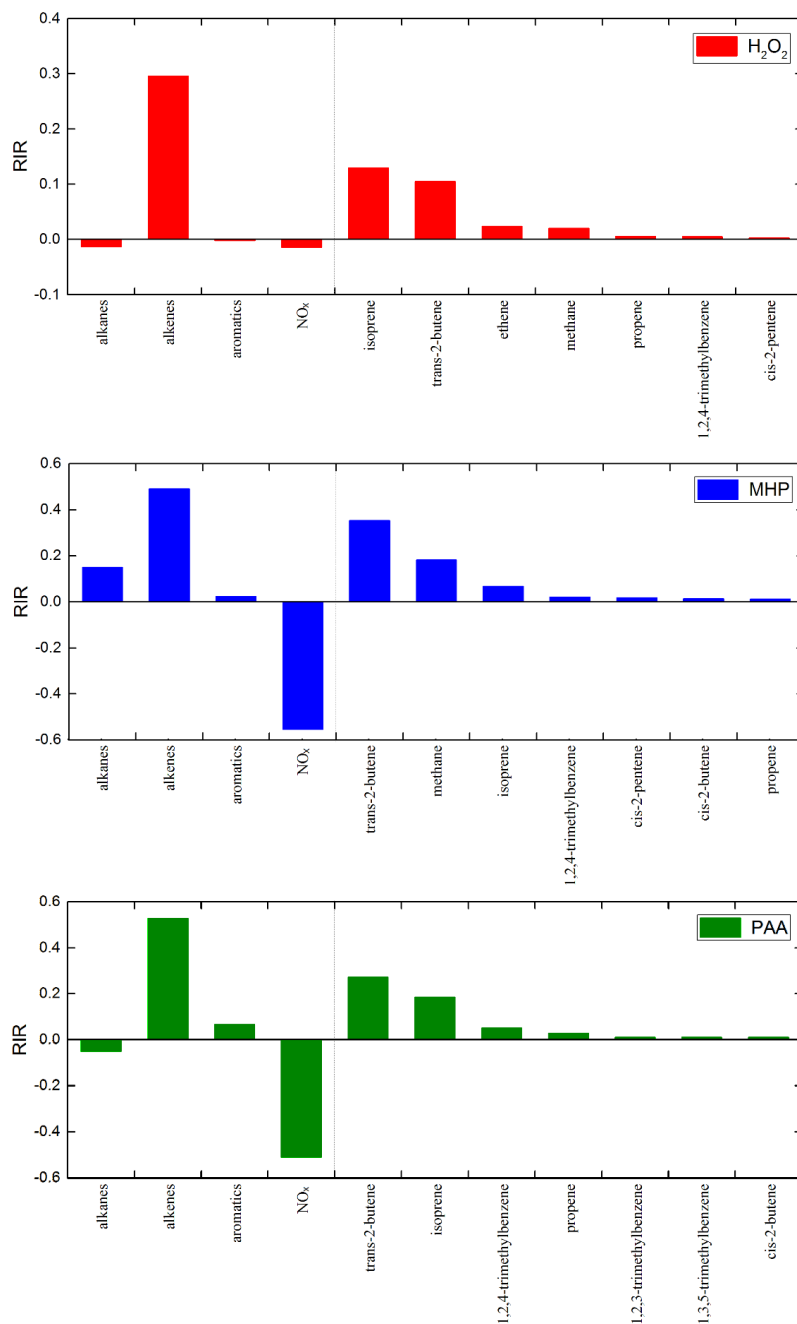


Figure 5. Sensitivity of production rate of atmospheric peroxides to major VOC precursor groups and individual VOC species for Phase I and Phase III.

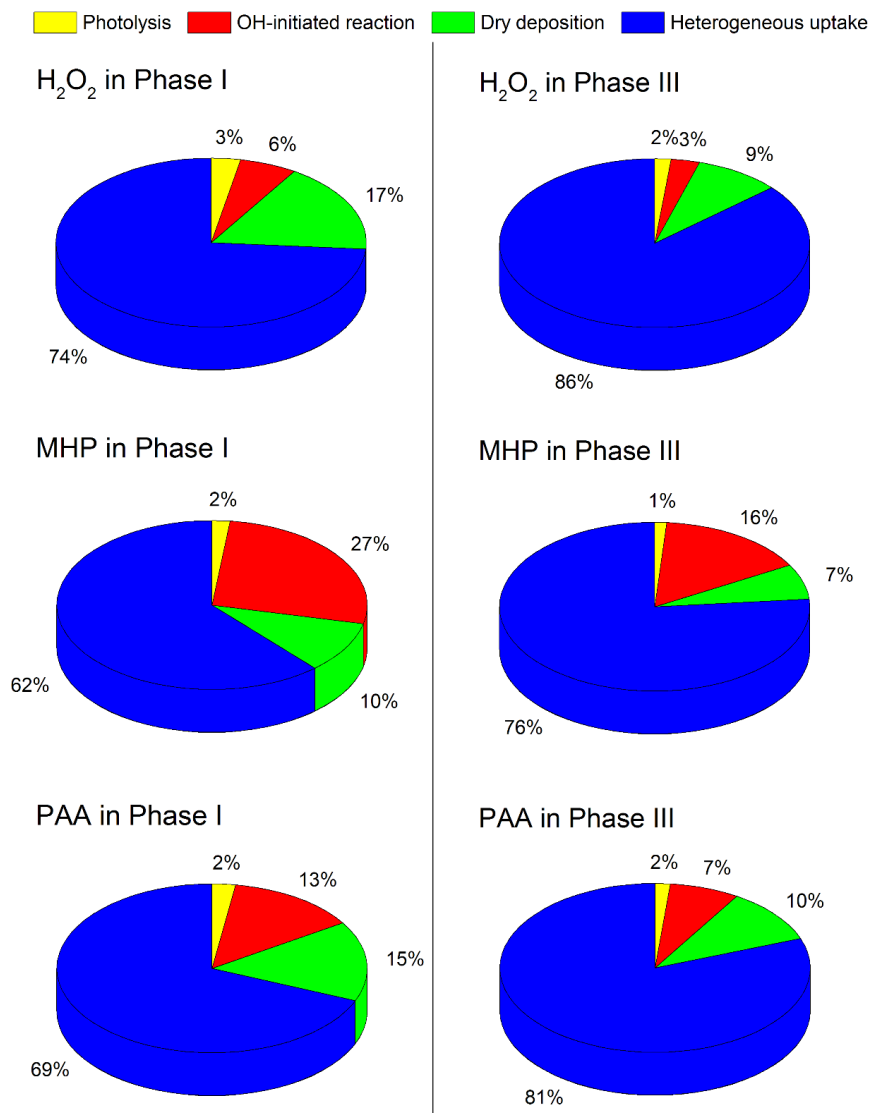


Figure 6. Contributions of each sink to H₂O₂, MHP and PAA destruction in the box model with the heterogeneous uptake by aerosols added during Phase I and Phase III.